



CHORUS

This is the accepted manuscript made available via CHORUS. The article has been published as:

Can Ab Initio Theory Explain the Phenomenon of Parity Inversion in ^{11}Be ?

Angelo Calci, Petr Navrátil, Robert Roth, Jérémy Dohet-Eraly, Sofia Quaglioni, and Guillaume Hupin

Phys. Rev. Lett. **117**, 242501 — Published 9 December 2016

DOI: [10.1103/PhysRevLett.117.242501](https://doi.org/10.1103/PhysRevLett.117.242501)

Can *ab initio* theory explain the phenomenon of parity inversion in ^{11}Be ?

Angelo Calci,^{1,*} Petr Navrátil,^{1,†} Robert Roth,² Jérémy Dohet-Eraly,^{1,‡} Sofia Quaglioni,³ and Guillaume Hupin^{4,5}

¹*TRIUMF, 4004 Wesbrook Mall, Vancouver, British Columbia, V6T 2A3, Canada*

²*Institut für Kernphysik, Technische Universität Darmstadt, 64289 Darmstadt, Germany*

³*Lawrence Livermore National Laboratory, P.O. Box 808, Livermore, California 94551, USA*

⁴*Institut de Physique Nucléaire, Université Paris-Sud, IN2P3/CNRS, F-91406 Orsay Cedex, France*

⁵*CEA, DAM, DIF, F-91297 Arpajon, France*

The weakly-bound exotic ^{11}Be nucleus, famous for its ground-state parity inversion and distinct $n+^{10}\text{Be}$ halo structure, is investigated from first principles using chiral two- and three-nucleon forces. An explicit treatment of continuum effects is found to be indispensable. We study the sensitivity of the ^{11}Be spectrum to the details of the three-nucleon force and demonstrate that only certain chiral interactions are capable of reproducing the parity inversion. With such interactions, the extremely large E1 transition between the bound states is reproduced. We compare our photo-disintegration calculations to conflicting experimental data and predict a distinct dip around the $3/2^-$ resonance energy. Finally, we predict low-lying $3/2^+$ and $9/2^+$ resonances that are not or not sufficiently measured in experiment.

Introduction. The theoretical understanding of exotic neutron-rich nuclei constitutes a tremendous challenge. These systems often cannot be explained by mean-field approaches and contradict the regular shell structure. The spectrum of ^{11}Be has some very peculiar features. The $1/2^+$ ground state (g.s.) is loosely bound by 502 keV with respect to the $n+^{10}\text{Be}$ threshold and is separated by only 320 keV from its parity-inverted $1/2^-$ partner [1], which would be the expected g.s. in the standard shell-model picture. Such parity inversion, already noticed by Talmi and Unna [2] in the early 1960s, is one of the best examples of disappearance of the $N = 8$ magic number with increasing neutron to proton ratio. The next ($n+n+^9\text{Be}$) break-up threshold, appears at 7.31 MeV [3], such that the rich resonance structure at low energies is dominated by the $n+^{10}\text{Be}$ dynamics. Peculiar is also the electric-dipole transition strength between the two bound states, which has attracted much attention since its first measurement in 1971 [4] and was remeasured in 1983 [5] and 2014 [6]. It is the strongest known transition between low-lying states, attributed to the halo character of ^{11}Be .

An accurate description of this complex spectrum is anticipated to be sensitive to the details of the nuclear force [7], such that a precise knowledge of the nucleon-nucleon (NN) interaction, desirably obtained from first principles, is crucial. Moreover, the inclusion of three-nucleon (3N) effects have been found to be indispensable for an accurate descriptions of nuclear systems [8, 9]. The chiral effective field theory (EFT) constitutes one of the most promising candidates for deriving the nuclear interaction. Formulated by Weinberg [10–12], it is based on the fundamental symmetries of QCD and uses pions and nucleons as relevant degrees of freedom. Within this theory NN, 3N and higher many-body interactions arise in a natural hierarchy [10–16]. The details of these interactions depend on the specific choices made during the construction. In particular the way the interactions are constrained to experimental data can have a strong impact [17].

In this work we tackle the question if *ab initio* calculations can provide an accurate description of the ^{11}Be spectrum and reproduce the experimental ground state. Pioneering *ab initio*

investigations of ^{11}Be did not account for the important effects of 3N forces and were incomplete in the treatment of either long- [18] or short-range [19, 20] correlations, both of which are crucial to arrive at an accurate description of this system.

In this Letter, we report the first complete *ab initio* calculations of the ^{11}Be nucleus using the framework of the no-core shell model with continuum (NCSMC) [21–23], which combines the capability to describe extended $n+^{10}\text{Be}$ configurations of Ref. [19, 20] with a robust treatment of many-body short-range correlations. We adopt a family of chiral interactions in which the NN component is constrained, in a traditional sense, to two-nucleon properties [24] and the 3N force is fitted in three- and sometimes four-body systems [25–28]. In addition, we also employ a newer chiral interaction, obtained from a simultaneous fit of NN and 3N components to nucleon-nucleon scattering data and selected properties of nuclei as complex as ^{25}O [29–31].

Many-body approach. The general idea of the NCSMC is to represent the A -nucleon wave function as the generalized cluster expansion [21–23]

$$|\Psi_A^{J^\pi T}\rangle = \sum_\lambda c_\lambda^{J^\pi T} |A\lambda J^\pi T\rangle + \sum_\nu \int dr r^2 \frac{\gamma_\nu^{J^\pi T}(r)}{r} \mathcal{A}_\nu |\Phi_{\nu r}^{J^\pi T}\rangle. \quad (1)$$

The first term consists of an expansion over the no-core shell model (NCSM) eigenstates of the compound system $|A\lambda J^\pi T\rangle$ (here ^{11}Be) indexed by λ . These states are expanded in a finite harmonic oscillator basis and thus well suited to cover the localized correlations of the A -body system, but are inappropriate to describe clustering and scattering properties. The latter properties are addressed by the second term corresponding to an expansion over the antisymmetrized cluster channels $\mathcal{A}_\nu |\Phi_{\nu r}^{J^\pi T}\rangle$ [20], which describe the two clusters (here $n+^{10}\text{Be}$) in relative motion. Here r denotes the relative distance of the clusters and ν is a collective index for the relevant quantum numbers. The expansion coefficients $c_\lambda^{J^\pi T}$ and the continuous relative-motion amplitudes $\gamma_\nu^{J^\pi T}(r)$ are obtained as a solution of the generalized eigenvalue problem derived by representing the Schrödinger equation in the model space of expan-

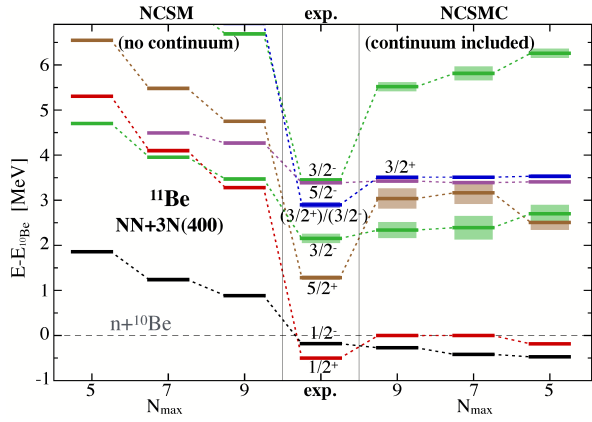


FIG. 1. (color online) Spectrum of ^{11}Be with respect to the $n+^{10}\text{Be}$ threshold. The NCSM (left) and NCSMC (right) calculations are carried out for different model-space sizes ($N_{\text{max}} = 5, 7, 9$). Light boxes of experimental and NCSMC spectra indicate resonance widths. Experimental energies taken from [1]. See text and supplemental material for details of the calculations [47].

sion (1) as detailed in Refs. [20, 22, 23]. The resulting NCSMC equations are solved by the coupled-channel R-matrix method on a Lagrange mesh [32–34]. The resonance energies and widths are deduced from the complex poles of the S -matrix, via the R -matrix approach extended to complex energies and momenta [35, 36].

The inclusion of the 3N force is computationally highly demanding and restricts the current application range of the NCSMC. For nuclei with $A > 5$ we rely on an on-the-fly computing of the uncoupled densities discussed in Ref. [37]. The present NCSMC calculations are performed including the first three eigenstates ($0^+, 2_1^+, 2_2^+$) of the ^{10}Be target, entering the cluster states in (1) and at least the first four negative- and three positive-parity eigenstates of ^{11}Be . Such eigenstates are obtained within the NCSM, except in the largest model spaces where, to reduce the dimension of the problem, we use the importance-truncated NCSM [38, 39].

Analysis of spectroscopy. We start by using an interaction and parameter set established in numerous studies [28, 37, 40–42] and investigate the convergence with respect to the model-space size N_{max} . We use the traditionally fitted chiral interaction where we choose the cutoff in the 3N regularization to be $\Lambda_{3N} = 400$ MeV, indicated by NN+3N(400). To accelerate the convergence of the many-body approach the interactions are softened via the similarity renormalization group (SRG) [43–45] as described in Refs. [28, 46] (see supplemental material for details [47]). Note that, both the SRG induced and initial 3N forces are treated explicitly at all steps of the calculations.

Without continuum effects, i.e., using the conventional NCSM a converged ^{11}Be spectrum cannot be obtained within accessible model spaces as demonstrated in Fig. 1. All states are unbound with respect to the $n+^{10}\text{Be}$ threshold. The positive-parity states converge especially slowly their excitation energy is too high compared to experiment. Once con-

tinuum effects are taken into account through the inclusion of the $n+^{10}\text{Be}$ cluster states in the model space, the convergence improves drastically, even though the computed threshold energy of $n+^{10}\text{Be}$ is not fully converged, yet. At $N_{\text{max}} = 9$ this energy is -58.4 MeV and increases by 2.3, 6.2 MeV for the $N_{\text{max}} = 7, 5$ model spaces, respectively. The extrapolated value of $-60.9(10)$ MeV is unbound with respect to the experimental energy of -64.976 MeV [3]. For the negative parity, the NCSMC achieves an overall quite reasonable description, especially for the three lowest states. On the other hand, the $1/2^+$ state is barely bound and the parity inversion of the bound states is not reproduced. Similarly the $3/2_1^-$ and $5/2^+$ states are inverted compared to experiment. The $3/2_2^-$ excitation energy is about 2 MeV larger than the experimental one. Other decay channels (and hence cluster states) presently not included may play a role at such high energies.

We first analyse the sensitivity of the spectrum to the 3N interaction in Fig. 2. From left to right we use exclusively the chiral NN interaction (including SRG induced 3N contributions), the 3N interaction with a 500 MeV cutoff, where parts of the two-pion exchange contribution are suppressed ($c_3 = 0$), and the full 3N contributions using the cutoffs $\Lambda_{3N} = 500, 450, 400$, and 350 MeV as introduced in [28]. The illustrated spectra are expected to show a similar convergence pattern as in the case of the NN+3N(400) interaction. The omitted SRG-induced beyond-3N contributions are expected to impact the ^{11}Be spectrum only for the NN+3N(500) interaction, while the remaining spectra are anticipated to be unaffected [27, 28, 46]. We find the two-pion exchange term to cause the dominant 3N effects in the ^{11}Be spectrum. The 3N interactions generally increase the excitation energies of both $3/2^-$ resonances, corresponding to the increase in excitation energy of the 2^+ states in ^{10}Be . Neither the inversion of the $1/2^+$ and $1/2^-$ states, nor that of the $3/2_1^-$ and $5/2^+$ states can be explained by the adopted 3N force versions. Decreasing the 3N cutoff initially reduces the bound-state splitting, but below $\Lambda_{3N} = 400$ MeV the influence of the 3N interaction is too strongly reduced such that the spectra approach the pure NN result. On the contrary, the converged spectrum with the simultaneously fitted NN+3N interaction, named $\text{N}^2\text{LO}_{\text{SAT}}$ [29], successfully achieves the parity inversions between the $3/2_1^-$ and $5/2^+$ resonances and, albeit marginally, for the bound states. The low-lying spectrum is significantly improved and agrees well with experiment, presumably due to the more accurate description of long-range properties caused by the fit of the interaction to radii of p-shell nuclei. On the other hand, the strongly overestimated splitting between the $3/2_2^-$ and $5/2^-$ states hints at deficiencies of this interaction, which might originate from a too large splitting of the $p_{1/2}$ - $p_{3/2}$ sub-shells.

In addition to the resonances observed in experiment all theoretical spectra predict a low-lying $9/2^+$ resonance suggested in Refs. [49, 50]. For the $\text{N}^2\text{LO}_{\text{SAT}}$ interaction the resonance energy is close to the one predicted by the Gamow shell model [51], although our *ab initio* calculations predict a broader width. Another interesting property is the position of

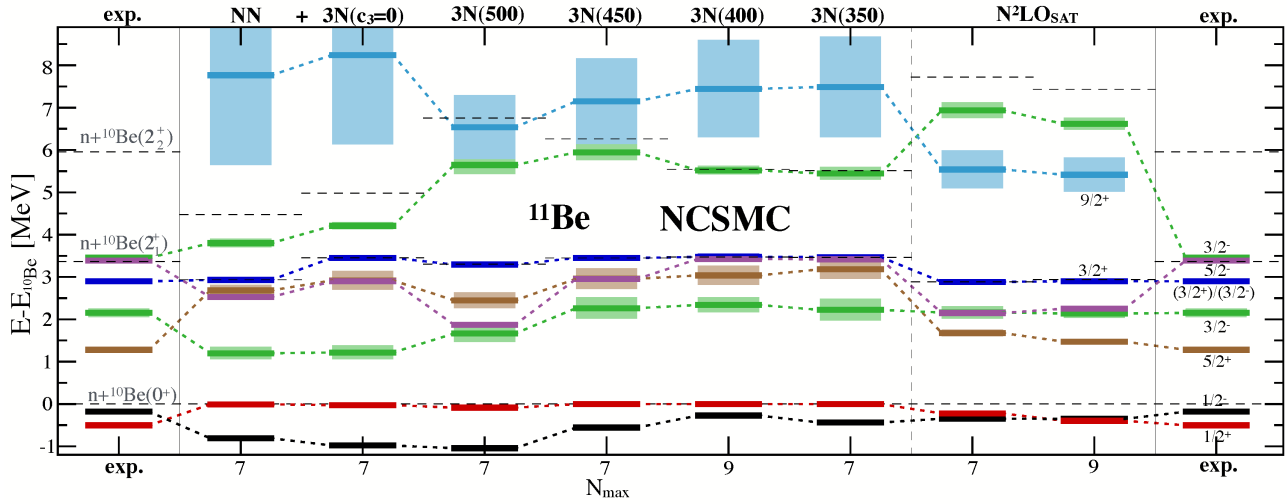


FIG. 2. (color online) NCSMC spectrum of ^{11}Be with respect to the $n+^{10}\text{Be}$ threshold. Dashed black lines indicate energies of the ^{10}Be states. Light boxes indicate resonance width. Experimental energies taken from [1, 48].

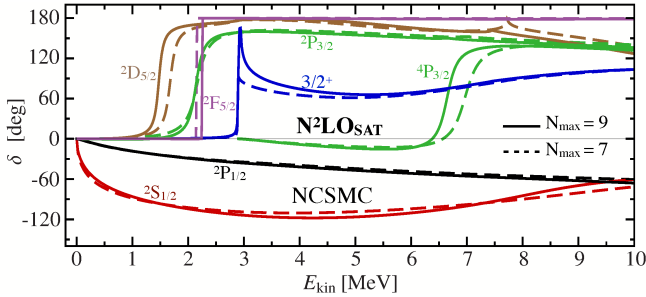


FIG. 3. (color online) The $n+^{10}\text{Be}$ phase shifts as function of the kinetic energy in the center-of-mass frame. NCSMC phase shifts for the $\text{N}^2\text{LO}_{\text{SAT}}$ interaction are compared for two model spaces indicated by N_{max} .

the $3/2^+$ resonance that is strongly influenced by the 2_1^+ state of ^{10}Be . For all theoretical calculations the energies of these correlated states are almost degenerate while in experiment the 2_1^+ state in ^{10}Be is about 470 keV above the tentative $3/2^+$ state and coincides with the $3/2^-$ and $5/2^-$ resonances.

Nuclear structure and reaction properties. Except for the two bound states, all the energy levels of Fig. 3 correspond to $n+^{10}\text{Be}$ scattering states. The corresponding phase shifts obtained with the $\text{N}^2\text{LO}_{\text{SAT}}$ interaction are presented in Fig. 3 (see supplemental material for further details [47]). The overall proximity of the $N_{\text{max}} = 7$ and 9 results confirms the good convergence with respect to the model space. The states observed in ^{11}Be are typically dominated by a single $n+^{10}\text{Be}$ partial wave but the illustrated eigenphase shifts of the $3/2^+$ state consist of a superposition of the $^4\text{S}_{3/2}$ and $^2\text{D}_{3/2}$ partial waves. The parity of this resonance is experimentally not uniquely extracted [1], while all *ab initio* calculations concordantly predict it to be positive. The bound-state energies as well as the resonance energies and widths for different interactions and both many-body approaches are summarized in Tab. I. In the case of the $\text{NN}+3\text{N}(400)$ interaction, however, the fast $3/2^+$

J^π	NCSMC				NCSMC-pheno		exp.	
	NN+3N(400)		$\text{N}^2\text{LO}_{\text{SAT}}$		$\text{N}^2\text{LO}_{\text{SAT}}$		E	Γ
	E	Γ	E	Γ	E	Γ	E	Γ
$1/2^+$	-0.001	-	-0.40	-	-0.50	-	-0.50	-
$1/2^-$	-0.27	-	-0.35	-	-0.18	-	-0.18	-
$5/2^+$	3.03	0.44	1.47	0.12	1.31	0.10	1.28	0.1
$3/2_1^+$	2.34	0.35	2.14	0.21	2.15	0.19	2.15	0.21
$3/2_2^+$	3.48	-	2.90	0.014	2.92	0.06	2.898	0.122
$5/2^-$	3.43	0.001	2.25	0.0001	3.30	0.0002	3.3874	<0.008
$3/2_2^-$	5.52	0.20	6.62	0.29	5.72	0.19	3.45	0.01
$9/2_2^-$	7.44	2.30	5.42	0.80	5.59	0.62	-	-

TABLE I. Excitation spectrum of ^{11}Be with respect to the $n+^{10}\text{Be}$ threshold. Energies and widths in MeV. The calculations are carried out at $N_{\text{max}} = 9$.

phase shift variation near the $n+^{10}\text{Be}(2_1^+)$ threshold does not correspond to a pole of the scattering matrix, such that this state is not a resonance in the conventional sense and a width could not be extracted reliably. The theoretical widths tend to overestimate the experimental value, but overall the agreement is reasonable, especially for the $\text{N}^2\text{LO}_{\text{SAT}}$ interaction. Experimentally only an upper bound could be determined for the $5/2^-$ resonance width and the theoretical calculations predict an extremely narrow resonance.

Although the bulk properties of the spectrum are already well described, accurate predictions of observables, such as electric-dipole (E1) transitions, which probe the structure of the nucleus, can be quite sensitive to the energies of the involved states with respect to the threshold. Based on our analysis, the discrepancies between the theoretical and experimental energy spectra can be mostly attributed to deficiencies in the nuclear force. Therefore, it can be beneficial to loosen the first-principles paradigm to remedy the insufficiencies in the nuclear force and provide accurate predictions for complex observables using the structure information of the *ab initio*

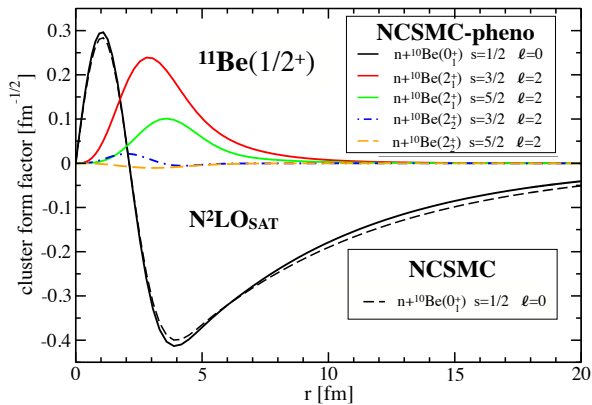


FIG. 4. (color online) Comparison of the cluster form factors with the $N^2\text{LO}_{\text{SAT}}$ interaction at $N_{\text{max}} = 9$. Note the coupling between the ^{10}Be target and neutron in the cluster state $|\Phi_{\nu,r}^{J\pi T}\rangle \sim [({}^{10}\text{Be} : I_1^{\pi_1} T_1) |n : 1/2^+ 1/2\rangle^{sT} Y_\ell(\hat{r})]^{J\pi T}$.

	NCSM	NCSMC	NCSMC-pheno	exp.
NN+3N(400)	0.0005	-	0.146	0.102(2) [6]
$N^2\text{LO}_{\text{SAT}}$	0.0005	0.127	0.117	

TABLE II. Reduced transition probability $B(E1: 1/2^- \rightarrow 1/2^+)$ between ^{11}Be bound states in $e^2\text{fm}^2$.

approach. In the following we use a phenomenology-inspired approach indicated by NCSMC-pheno that has been already applied in Refs. [36, 52]. In this approach we adjust the ^{10}Be and ^{11}Be excitation energies of the NCSM eigenstates entering expansion (1) to reproduce the experimental energies of the first low-lying states. Note that, the obtained NCSMC-pheno energies are fitted to experiment while the theoretical widths, quoted in Tab. I, are predictions.

An intuitive interpretation of the ^{11}Be g.s. wave function, is provided in Fig. 4 by the overlap of the full solution for the g.s. $|\Psi_{\nu}^{J\pi T}\rangle$ in (1) with the cluster portion $|\Phi_{\nu,r}^{J\pi T}\rangle$ given by $r \cdot \langle \Phi_{\nu,r}^{J\pi T} | \mathcal{A}_{\nu} | \Psi_{\nu}^{J\pi T} \rangle$. A clearly extended halo-structure beyond 20 fm can be identified for the S-wave of the $^{10}\text{Be}(0^+)+n$ relative motion. The phenomenological energy adjustment only slightly influences the asymptotic behavior of the S-wave, as seen by comparing the solid and dashed black curves, while other partial waves are even indistinguishable on the plot resolution. The corresponding spectroscopic factors for the NCSMC-pheno approach, obtained by integrating the squared cluster form factors in Fig. 4 are: $S = 0.90$ (S-wave) and $S=0.16$ (D-wave). The S-wave asymptotic normalization coefficient is $0.786 \text{ fm}^{-1/2}$.

The $B(E1)$ transitions are summarized in Tab. II. Calculations without continuum effects predict the wrong g.s. and underestimate the E1 strength by several orders of magnitude. For the NCSMC calculations with the NN+3N(400) interaction the $1/2^+$ state is very weakly bound leading to an unrealistic E1 transition. The $N^2\text{LO}_{\text{SAT}}$ interaction successfully reproduces the strong E1 transition, albeit the latest measurement [6] is slightly overestimated, even after the phenomeno-

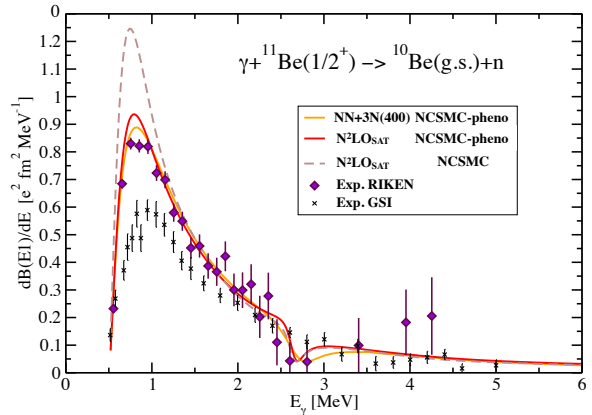


FIG. 5. (color online) Dipole strength distribution $dB(E1)/dE$ of the photodisintegration process as function of the photon energy. Theoretical dipole strength distribution for two chiral interaction with (solid) and without (dashed) the phenomenological energy adjustment are compared to the experimental measurements at GSI [55, 56] (black dots) and RIKEN [56–58] (violet dots).

logical energy adjustment. There might be small effects arising from a formally necessary SRG evolution of the transition operator. Works along these lines for ^4He suggest a slight reduction of the dipole strength [53, 54]. A similar effect would bring the calculated E1 transition in better agreement with experiment [6].

Finally we study the photodisintegration of the ^{11}Be g.s. into $n+^{10}\text{Be}$ in Fig. 5. This is proportional to dipole strength distribution $dB(E1)/dE$. In all approaches, a peak of non-resonant nature (see Fig. 3) is present at about 800 keV above the $n+^{10}\text{Be}$ threshold, particularly pronounced in the $3/2^-$ partial wave. The strong peak for the NCSMC with the $N^2\text{LO}_{\text{SAT}}$ interaction is caused by the slightly extended S-wave tail in Fig. 4 and hence the underestimated binding energy of the $1/2^+$ state. The theoretical predictions are compared to indirect measurements of the photodissociation process extracted from the scattering experiments of ^{11}Be on lead [56–58] and carbon [55, 56] targets. Our phenomenological adjusted calculations show good agreement with the RIKEN data [56–58]. Based on the analysis in Ref. [53, 54], it is doubtful that the missing SRG evolution of the E1-transition operator could explain the $\sim 30\%$ discrepancy with the GSI data [55, 56]. A dip in the dipole strength distribution is present at about 2.7 MeV, due to the $3/2_1^-$ resonance. At this energy, the E1 matrix element between the ^{11}Be g.s. wave function and the $3/2^-$ partial wave of the $n+^{10}\text{Be}$ scattering wave function changes its sign. Due to large uncertainties the experimental data neither confirm nor exclude such a dip. A similar feature, but much less pronounced, can be noticed in microscopic cluster calculations [59] (see supplemental material for details [47]).

Conclusions. We have demonstrated that the inclusion of continuum effects is crucial for a description of the ^{11}Be system and, further that the spectrum is extremely sensitive to the details of the nuclear NN+3N interactions and constitutes an important benchmark for future forces. In particular, the parity inversion of the bound states could only be achieved by

the $N^2\text{LO}_{\text{SAT}}$ interaction that provides accurate predictions of nuclear radii and matter saturation properties [29, 30]. An interesting related endeavour is the investigation of the mirror system $p+^{10}\text{C}$. New experiments have been performed for the elastic scattering process [60] that will be analysed with the NCSMC.

Prepared in part by LLNL under Contract DE-AC52-07NA27344. Supported by the U.S. Department of Energy, Office of Science, Office of Nuclear Physics, under Work Proposal No. SCW1158, by the NSERC Grants No. SAPIN-2016-00033 and by the Deutsche Forschungsgemeinschaft through SFB 1245. TRIUMF receives federal funding via a contribution agreement with the National Research Council of Canada. Computing support came from the LLNL institutional Computing Grand Challenge Program, from an INCITE Award on the Titan supercomputer of the Oak Ridge Leadership Computing Facility (OLCF) at ORNL, the LOEWE-CSC Frankfurt, the computing center of the TU Darmstadt (LICHT-ENBERG) and from Calcul Quebec and Compute Canada.

* calci@triumf.ca
† navratil@triumf.ca
‡ Present address: Istituto Nazionale di Fisica Nucleare, Sezione di Pisa, Largo B. Pontecorvo 3, I-56127 Pisa, Italy.

[1] D. Tilley, J. Kelley, J. Godwin, D. Millener, J. Purcell, C. Sheu, and H. Weller, *Nucl. Phys. A* **745**, 155 (2004).
[2] I. Talmi and I. Unna, *Phys. Rev. Lett.* **4**, 469 (1960).
[3] M. Wang, G. Audi, A. H. Wapstra, F. G. Kondev, M. MacCormick, X. Xu, and B. Pfeiffer, *Chinese Physics C* **36**, 1603 (2012).
[4] S. S. Hanna, K. Nagatani, W. R. Harris, and J. W. Olness, *Phys. Rev. C* **3**, 2198 (1971).
[5] D. J. Millener, J. W. Olness, E. K. Warburton, and S. S. Hanna, *Phys. Rev. C* **28**, 497 (1983).
[6] E. Kwan, C. Wu, N. Summers, G. Hackman, T. Drake, C. Andreou, R. Ashley, G. Ball, P. Bender, A. Boston, H. Boston, A. Chester, A. Close, D. Cline, D. Cross, R. Dunlop, A. Finlay, A. Garnsworthy, A. Hayes, A. Laffoley, T. Nano, P. Navratil, C. Pearson, J. Pore, S. Quaglioni, C. Svensson, K. Starosta, I. Thompson, P. Voss, S. Williams, and Z. Wang, *Phys. Lett. B* **732**, 210 (2014).
[7] A. Calci and R. Roth, *Phys. Rev. C* **94**, 014322 (2016).
[8] S. C. Pieper and R. B. Wiringa, *Ann. Rev. Nucl. Part. Sci.* **51**, 53 (2001).
[9] P. Navrátil, V. G. Gueorguiev, J. P. Vary, W. E. Ormand, and A. Nogga, *Phys. Rev. Lett.* **99**, 042501 (2007).
[10] S. Weinberg, *Physica A: Statistical Mechanics and its Applications* **96**, 327 (1979).
[11] S. Weinberg, *Phys. Lett. B* **251**, 288 (1990).
[12] S. Weinberg, *Nucl. Phys. B* **363**, 3 (1991).
[13] C. Ordóñez, L. Ray, and U. van Kolck, *Phys. Rev. Lett.* **72**, 1982 (1994).
[14] U. van Kolck, *Phys. Rev. C* **49**, 2932 (1994).
[15] E. Epelbaum, A. Nogga, W. Glöckle, H. Kamada, U.-G. Meißner, and H. Witała, *Phys. Rev. C* **66**, 064001 (2002).
[16] E. Epelbaum, *Prog. Part. Nucl.* **57**, 654 (2006).
[17] B. D. Carlsson, A. Ekström, C. Forssén, D. F. Strömberg, G. R. Jansen, O. Lilja, M. Lindby, B. A. Mattsson, and K. A. Wendt,

Phys. Rev. X **6**, 011019 (2016).
[18] C. Forssén, P. Navrátil, W. E. Ormand, and E. Caurier, *Phys. Rev. C* **71**, 044312 (2005).
[19] S. Quaglioni and P. Navrátil, *Phys. Rev. Lett.* **101**, 092501 (2008).
[20] S. Quaglioni and P. Navrátil, *Phys. Rev. C* **79**, 044606 (2009).
[21] S. Baroni, P. Navrátil, and S. Quaglioni, *Phys. Rev. Lett.* **110**, 022505 (2013).
[22] S. Baroni, P. Navrátil, and S. Quaglioni, *Phys. Rev. C* **87**, 034326 (2013).
[23] P. Navrátil, S. Quaglioni, G. Hupin, C. Romero-Redondo, and A. Calci, *Phys. Scr.* **91**, 053002 (2016).
[24] R. Machleidt and D. R. Entem, *Phys. Rep.* **503**, 1 (2011).
[25] P. Navrátil, *Few Body Syst.* **41**, 117 (2007).
[26] D. Gazit, S. Quaglioni, and P. Navrátil, *Phys. Rev. Lett.* **103**, 102502 (2009).
[27] R. Roth, S. Binder, K. Vobig, A. Calci, J. Langhammer, and P. Navrátil, *Phys. Rev. Lett.* **109**, 052501 (2012).
[28] R. Roth, A. Calci, J. Langhammer, and S. Binder, *Phys. Rev. C* **90**, 024325 (2014).
[29] A. Ekström, G. R. Jansen, K. A. Wendt, G. Hagen, T. Papenbrock, B. D. Carlsson, C. Forssén, M. Hjorth-Jensen, P. Navrátil, and W. Nazarewicz, *Phys. Rev. C* **91**, 051301(R) (2015).
[30] G. Hagen, A. Ekstrom, C. Forssen, G. R. Jansen, W. Nazarewicz, T. Papenbrock, K. A. Wendt, S. Bacca, N. Barnea, B. Carlsson, C. Drischler, K. Hebeler, M. Hjorth-Jensen, M. Miorelli, G. Orlandini, A. Schwenk, and J. Simonis, *Nat. Phys.* **12**, 186 (2016).
[31] M. Miorelli, S. Bacca, N. Barnea, G. Hagen, G. R. Jansen, G. Orlandini, and T. Papenbrock, (2016), arXiv:1604.05381 [nucl-th].
[32] P. Descouvemont and D. Baye, *Reports on Progress in Physics* **73**, 036301 (2010).
[33] M. Hesse, J. Roland, and D. Baye, *Nucl. Phys. A* **709**, 184 (2002).
[34] D. Baye, J. Goldbeter, and J.-M. Sparenberg, *Phys. Rev. A* **65**, 052710 (2002).
[35] B. I. Schneider, *Phys. Rev. A* **24**, 1 (1981).
[36] J. Dohet-Eraly, P. Navrátil, S. Quaglioni, W. Horiuchi, G. Hupin, and F. Raimondi, *Phys. Lett. B* **757**, 430 (2016).
[37] G. Hupin, J. Langhammer, P. Navrátil, S. Quaglioni, A. Calci, and R. Roth, *Phys. Rev. C* **88**, 054622 (2013).
[38] R. Roth, *Phys. Rev. C* **79**, 064324 (2009).
[39] R. Roth and P. Navrátil, *Phys. Rev. Lett.* **99**, 092501 (2007).
[40] J. Langhammer, P. Navrátil, S. Quaglioni, G. Hupin, A. Calci, and R. Roth, *Phys. Rev. C* **91**, 021301(R) (2015).
[41] S. Binder, J. Langhammer, A. Calci, and R. Roth, *Phys. Lett. B* **736**, 119 (2014).
[42] R. Roth, J. Langhammer, S. Binder, and A. Calci, *J. Phys.: Conf. Ser.* **403**, 012020 (2012).
[43] F. Wegner, *Ann. Phys. (Leipzig)* **506**, 77 (1994).
[44] S. K. Bogner, R. J. Furnstahl, and R. J. Perry, *Phys. Rev. C* **75**, 061001(R) (2007).
[45] S. Szpigel and R. J. Perry, in *Quantum Field Theory. A 20th Century Profile*, edited by A. N. Mitra (Hindustan Publishing Co., New Delhi, 2000).
[46] R. Roth, J. Langhammer, A. Calci, S. Binder, and P. Navrátil, *Phys. Rev. Lett.* **107**, 072501 (2011).
[47] See Supplemental Material [url], which includes Refs. [61–64].
[48] J. Kelley, E. Kwan, J. Purcell, C. Sheu, and H. Weller, *Nucl. Phys. A* **880**, 88 (2012).
[49] N. Aoi, K. Yoneda, H. Miyatake, H. Ogawa, Y. Yamamoto, E. Ideguchi, T. Kishida, T. Nakamura, M. Notani, H. Sakurai,

- T. Teranishi, H. Wu, S. Yamamoto, Y. Watanabe, A. Yoshida, and M. Ishihara, *Nucl. Phys. A* **616**, 181 (1997).
- [50] Y. Hirayama, T. Shimoda, H. Izumi, H. Yano, M. Yagi, A. Hatakeyama, C. Levy, K. Jackson, and H. Miyatake, *Nucl. Phys. A* **738**, 201 (2004).
- [51] K. Fosse, W. Nazarewicz, Y. Jaganathen, N. Michel, and M. Płoszajczak, *Phys. Rev. C* **93**, 011305 (2016).
- [52] F. Raimondi, G. Hupin, P. Navrátil, and S. Quaglioni, *Phys. Rev. C* **93**, 054606 (2016).
- [53] M. D. Schuster, S. Quaglioni, C. W. Johnson, E. D. Jurgenson, and P. Navrátil, *Phys. Rev. C* **90**, 011301(R) (2014).
- [54] M. D. Schuster, S. Quaglioni, C. W. Johnson, E. D. Jurgenson, and P. Navrátil, *Phys. Rev. C* **92**, 014320 (2015).
- [55] R. Palit, P. Adrich, T. Aumann, K. Boretzky, B. V. Carlson, D. Cortina, U. Datta Pramanik, T. W. Elze, H. Emling, H. Geissel, M. Hellström, K. L. Jones, J. V. Kratz, R. Kulessa, Y. Leifels, A. Leistenschneider, G. Münzenberg, C. Nociforo, P. Reiter, H. Simon, K. Sümmerer, and W. Walus (LAND/FRS Collaboration), *Phys. Rev. C* **68**, 034318 (2003).
- [56] T. Aumann and T. Nakamura, *Phys. Scr.* **2013**, 014012 (2013).
- [57] T. Nakamura, S. Shimoura, T. Kobayashi, T. Teranishi, K. Abe, N. Aoi, Y. Doki, M. Fujimaki, N. Inabe, N. Iwasa, K. Katori, T. Kubo, H. Okuno, T. Suzuki, I. Tanihata, Y. Watanabe, A. Yoshida, and M. Ishihara, *Phys. Lett. B* **331**, 296 (1994).
- [58] N. Fukuda, T. Nakamura, N. Aoi, N. Imai, M. Ishihara, T. Kobayashi, H. Iwasaki, T. Kubo, A. Mengoni, M. Notani, H. Otsu, H. Sakurai, S. Shimoura, T. Teranishi, Y. X. Watanabe, and K. Yoneda, *Phys. Rev. C* **70**, 054606 (2004).
- [59] P. Descouvemont, *Nucl. Phys. A* **615**, 261 (1997).
- [60] A. Kumar, R. Kanungo, A. Calci, P. Navrátil et al. in preparation.
- [61] H. Hergert, S. Binder, A. Calci, J. Langhammer, and R. Roth, *Phys. Rev. Lett.* **110**, 242501 (2013).
- [62] H. Hergert, S. K. Bogner, S. Binder, A. Calci, J. Langhammer, R. Roth, and A. Schwenk, *Phys. Rev. C* **87**, 034307 (2013).
- [63] A. Cipollone, C. Barbieri, and P. Navrátil, *Phys. Rev. Lett.* **111**, 062501 (2013).
- [64] E. Gebrerufael, A. Calci, and R. Roth, *Phys. Rev. C* **93**, 031301 (2016).